Research Square

Preprints are preliminary reports that have not undergone peer review.
They should not be considered conclusive, used to inform clinical practice,
or referenced by the media as validated information.

Bose-Einstein condensation and collective Bogoliubov excitations of microwave photons in superconducting quantum electrodynamics circuits

Valentina Di Meo

valentina.dimeo@spin.cnr.it

Institute for Superconductors, Innovative materials, and devices - CNR SPIN https://orcid.org/0000-0001-9622-1817

Patrick Navez

Université de Montpellier

Berardo Ruggiero

Institute of Applied Sciences and Intelligent Systems

Claudio Gatti

INFN https://orcid.org/0000-0003-3676-1787

Fabio Chiarello

CNR https://orcid.org/0000-0002-7487-2827

Alessandro D'Elia

INFN https://orcid.org/0000-0002-6856-7703

Alessio Rettaroli

INFN

Giorgio Brida

INRIM

Emanuele Enrico

INRiM https://orcid.org/0000-0002-2125-5200

Luca Fasolo

Istituto Nazionale di Ricerca Metrologica https://orcid.org/0000-0002-7537-7772

Mikahil Fistul

Theoretische Physik III, Ruhr-Universit¨at Bochum

Ilya Eremin

Ruhr-Universität Bochum https://orcid.org/0000-0003-0557-8015

Alexandre Zagoskin

Loughborough University https://orcid.org/0000-0002-1189-5116

Paolo Vanacore

Area Territoriale di Ricerca Napoli 1 (CNR ATdR NA1)

Paolo Silvestrini
Department of Mathematics and Physics, University of Campania ”Luigi Vanvitelli”
Mikhail Lisitskiy
Institute for Superconductors, Innovative materials, and devices - CNR SPIN

Article

Keywords:

Posted Date: August 7th, 2026

DOI: https://doi.org/10.21203/rs.3.rs-10420335/v1

License: This work is licensed under a Creative Commons Attribution 4.0 International License.
Read Full License

Additional Declarations: There is **NO** Competing Interest.

Bose-Einstein condensation and collective Bogoliubov excitations of microwave photons in superconducting quantum electrodynamics circuits

Patrick Navez[1], Valentina Di Meo*[2], Berardo Ruggiero[3], Claudio Gatti[4], Fabio Chiarello[5], Alessandro D'Elia[4], Alessio Rettaroli[4], Giorgio Brida[6], Emanuele Enrico[6], Luca Fasolo[6], Mikhail Fistul[7], Ilya Eremin[7], Alexandre Zagoskin[8], Paolo Vanacore[9], Paolo Silvestrini[10], and Mikhail Lisitskiy*[2]

[1]Université de Montpellier, 163 rue Auguste Broussonnet F-34090 Montpellier, France

[2]Institute for Superconductors, Innovative materials, and devices - CNR SPIN, Via Campi Flegrei 34, I-80078, Italy

[3]Institute of Applied Sciences and Intelligent Systems - CNR ISASI, Via Campi Flegrei 34, I-80078, Italy

[4]National Laboratory of Frascati LNF, National Institute of Nuclear Physics - INFN, Via Enrico Fermi 54, I- 00044 , Frascati (Rome), Italy

[5]Institute for Photonics and Nanotechnologies - CNR IFN, Via del Fosso del Cavaliere 100, I-00133 Roma RM

[6]National Institute of Metrological Research, INRiM, Strada delle Cacce 91, I-10135 , Turin, Italy

[7] Theoretische Physik III, Ruhr-Universität Bochum, Bochum D-44801, Germany

[8]Loughborough University, LE11 3TU, Loughborough, United Kingdom

[9]Area Territoriale di Ricerca Napoli 1 (CNR ATdR NA1) Via P. Castellino 111, 80131, Napoli

[10]Department of Mathematics and Physics, University of Campania "Luigi Vanvitelli", Viale Lincoln 5, I- 81100 Caserta, Italy

Abstract

The seminal phenomenon of the Bose-Einstein condensation has been observed on a large variety of physical platforms, e.g., superfluid helium, fermions with attractive interactions, quasiparticles in solids, and ultracold atomic gases. Recently, the Bose–Einstein condensation of non-interacting photons in an optical microcavity has been confirmed experimentally. Here, we report the experimental observation of Bose-Einstein like condensation and collective Bogoliubov excitations in a low dissipative microwave resonator with embedded superconducting quantum network composed of multiple flux qubits. Under strong coherent pumping the resonator mode becomes macroscopically populated, giving rise to hybridized photon–qubit collective modes. The Bogoliubov-like col-

*Corresponding authors: Valentina Di Meo (valentina.dimeo@spin.cnr.it) and Mikhail Lisitskiy (mikhail.lisitskiy@spin.cnr.it)

lective excitations appearing in a response to a nearby-frequency probe tone, accompanied by pronounced bistability and hysteresis in the measured transmission coefficient, provide the first experimental evidence of a Bose–Einstein–like condensate of microwave photons on a superconducting circuit platform. A theoretical framework based on Gross-Pitaevskii formalism and taking into account the ac Stark effect inducing the effective interaction between photons, quantitatively reproduces the experimental observations and identifies the regime of appearance of microwave Bogoliubov excitations. These results establish a proof of principle for exploiting driven collective states in superconducting circuits as a platform for quantum-limited microwave detection and engineered many-body photonic systems for quantum information processing.

Introduction

For a long time, collective quantum phenomena associated with the Bose–Einstein condensation (BEC) have attracted a great attention of scientific community [1, 2, 3], and it has been observed in a variety of different physical systems such as superfluid helium [2, 3], ultracold atomic gases with magnetic and laser traps [4, 5, 6, 7], fermions with an extremely strong attractive interaction demonstrating the superconducting BEC [1, 8, 9], and quasiparticles such as magnons, excitons, in solids [10, 11, 12, 13]. These systems have provided the main experimental platforms for exploring macroscopic quantum coherence and the emergence of collective excitation spectra in condensed matter physics.

In contrast, collective quantum effects involving photons, i.e., bosonic excitations in electromagnetic resonators, have only recently become a central subject of investigation, and the BEC of non-interacting photons trapped in an optical microcavity has been confirmed experimentally [14]. In parallel, a growing interest in *microwave photonics* is largely driven by the rapid development of superconducting quantum

technologies, where microwave photons play a crucial role in mediating qubits interactions, storing quantum information, and enabling the operation of quantum processors [15, 16]. Understanding whether microwave photon fields can sustain collective quantum states analogous to BECs, together with their associated excitation spectra, represents an important challenge at the interface between many-body quantum physics and emerging quantum technologies. In particular, among the collective phenomena relevant to driving quantum systems, Bogoliubov excitations, which arise in Bose–Einstein condensates, play a central role in describing the elementary modes of interacting quantum systems that emerge above a macroscopically occupied state in the presence of interactions and nonlinearity. While such modes are well theoretically investigated in many areas of condensed matter, atomic and photon physics [17, 18], their experimental observation and control in superconducting quantum networks remain largely unexplored. In solid state qubit devices, Bogoliubov excitations can be considered as a relevant phenomena for quantum-limited detection and nonlinear response of microwave photons. In these platforms, strong coherent pumping can macroscopically populate a resonator mode, leading to a Bose-Einstein like condensate of microwave photons in a driven-dissipative sense, that is, without implying an equilibrium thermodynamic phase transition. In this regime, the relevant excitations are no longer those of independent photons or isolated qubits, but hybrid collective photon-qubit modes that can dominate the nonlinear response of the system.

Low dissipative superconducting resonators with embedded superconducting qubits networks (SQNs), operating in the macroscopic quantum electrodynamics (QED) regime, provide an attractive platform to investigate collective microwave photon–matter interactions at the quantum level [19, 20, 21, 22, 23, 24]. In this context, the rapid development of quantum technologies has stimulated intense research on SQNs, in which many interacting qubits operate coherently on macroscopic scales and enable applications ranging from quantum information processing to sensitive photon de-

tection [25, 26]. When an SQN is coupled, even weakly, to a high-quality resonator, the resonator mediates effective qubit–qubit interactions [24, 27, 28] and can foster collective quantum states [29, 30]. Moreover, through ac Stark effect, the frequencies of qubits vary with the number of photons, and, in turn, an SQN induces an effective Kerr nonlinearity and photon–photon interactions [31, 32]. These features make resonators with embedded SQNs particularly appealing for realizing quantum-limited detectors, in which the collective dynamics can transduce weak microwave signals through emergent many-body excitation modes [28, 33, 34]. Previous experimental and theoretical studies have explored nonlinear interactions and dynamics, bistability, and parametric effects in superconducting circuits, including Josephson junction arrays [35, 36], Josephson transmission lines [37, 38] used as a basic design of parametric Josephson traveling-wave amplifiers [39, 40, 41], and single-qubit circuit QED systems [42, 43, 44, 45, 46]. In these experiments nonlinear response typically originates from the intrinsic anharmonicity of individual elements or from externally engineered parametric driving and is often well described within single-emitter or few-mode frameworks. However, experimental demonstrations of the collective states in the microwave photon field have so far been limited, and the BECs in the microwave photon fields have not been observed.

In this work, we aim at the investigation of the collective quantum states in the microwave photon mode pumped by a strong microwave drive in a QED device where the non-linearity has been provided by an SQN embedded in low-dissipative resonators. In this regime, the macroscopically populated photon field behaves as a Bose-Einstein like condensate and the relevant excitations become hybridized photon–qubit collective modes. We report the observation of Bogoliubov-like collective excitations in the response to a nearby-frequency probe tone, accompanied by pronounced bistability and hysteresis in the measured transmission coefficient, providing, to our knowledge, the first experimental evidence of a Bose–Einstein–like condensate

of microwave photons on a superconducting circuit platform. We further develop a theoretical framework based on the time-dependent nonlinear Gross-Pitaevskii like equation which quantitatively reproduces the experimental results.

Results

Physical device and experimental setup

The device schematically shown in Fig. 1 integrates two resonators (T-resonator and R-resonator) interacting through an SQN that serves as a collective/nonlinear coupling element. The SQN consists of 10 capacitively-shunted superconducting flux qubits, each containing a superconducting loop interrupted by 3 Josephson junctions [47, 48]. In the implemented architecture, the SQN is inductively coupled to the T resonator and capacitively coupled to the R resonator by the interdigital gap capacitor. The device electromagnetic mode is characterized by the resonant frequency $f_r \simeq 7.7GHz$ and an external coupling quality factor $Q_c \simeq 10^5$ (see Methods, section A and D).

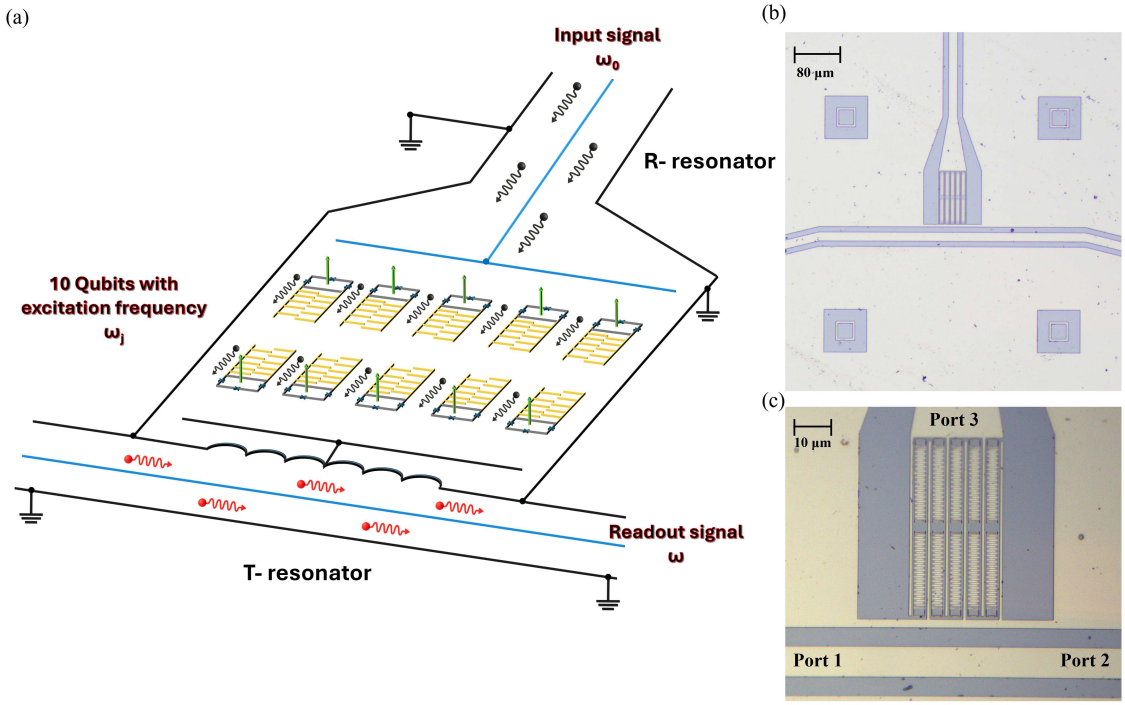


Figure 1: (a) Schematic of the device integrating two microwave resonators (T and R) coupled through an SQN including ten superconducting flux qubits with excitation frequencies ω_j. A microwave tone of frequency ω_0 (pump signal) is applied as input at Port 3 (see panel (c)), and the transmitted (readout) signal of frequency ω is measured at the output between Port 1 and Port 2. The green arrows represent the direction of the magnetic field. (b), (c) Optical image of the fabricated SQN and its coupling to the resonator. Scale bars: 80 μm (b) and 10 μm (c).

The T-resonator, connected between Ports 1 and 2, is terminated at both ends by two 5fF capacitors. The R-resonator, connected to Port 3, is terminated by a 5fF capacitor at one end and is capacitively coupled to the flux-qubit array at the other end. This T-shaped configuration provides inductive coupling between the T-resonator and the qubit array, capacitive coupling between the R-resonator and the qubits, and suppresses direct parasitic coupling between the two resonators. Details of

the fabrication of both resonators and the SQN are provided in the Methods (Section A); optical images of the SQN coupled to the T- and R- resonators are shown in Fig. 1, panels b) and c). The device layout is shown in the Supplementary Material.

First, we performed single-tone measurements of scattering parameters between the different ports. After that, two-tone spectroscopy measurements were carried out by measuring the frequency dependence of the transmission coefficient $S_{21}(f)$, of the T resonator (from port 1 to port 2) while injecting a second microwave tone into the R resonator at port 3. We denote the probe (first-tone) and pump (second-tone) frequencies, f and f_{pump}, accordingly. The pump frequency was swept over a narrow region around the resonance of the R resonator. Unless otherwise stated, measurements were carried out at zero applied magnetic field. The pump power was varied from -110 dBm to -60 dBm. All experiments were carried out at 15 mK temperature. The description of the experimental setup, together with further details, is provided in the Supplementary Material.

Two-tone spectroscopy: Measurements of the Transmission Coefficient

In Fig. 2 the representative spectra of the probe transmission magnitude, $|S_{21}|$ as a function of the probe frequency f, for three closely spaced values of the pump power, are presented. In all cases, the spectra display pronounced resonant dips. Their exceptionally small linewidth indicates a large external coupling quality factor, Q_c, for the studied system.

A key experimental result is a systematic *red shift* of the resonance, i.e., a displacement of the dip towards lower frequencies as the pump power is increased. This shift becomes markedly stronger once the pump power P_{pump} exceeds a threshold value P_{cr} (Fig. 2(b). Notably, when P_{pump} is only slightly above P_{cr}, the resonance remains very narrow (Fig. 2(b,c).

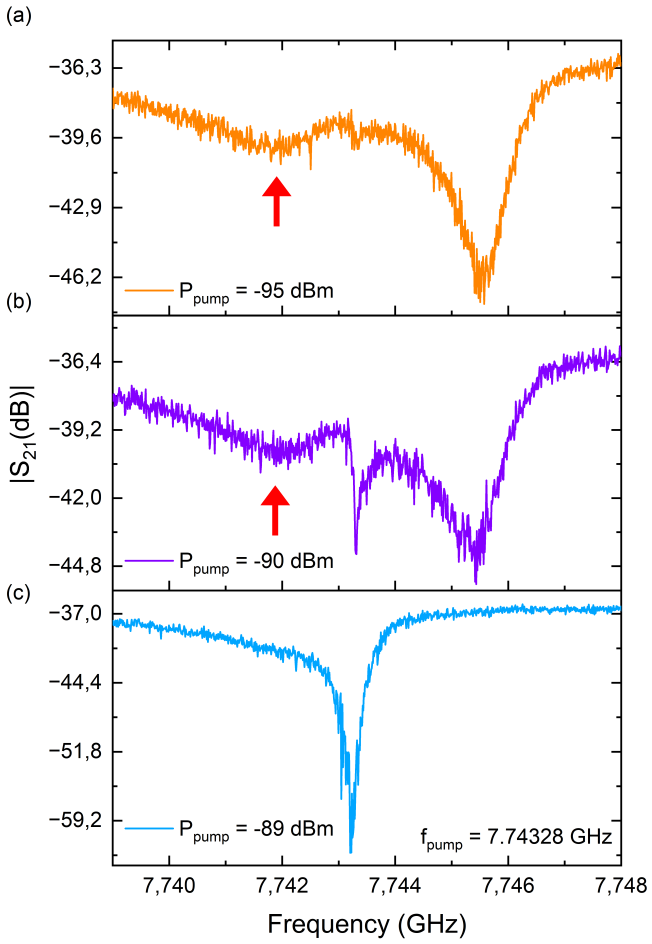


Figure 2: The dependence of the transmission coefficient $|S_{21}|$ on the probe frequency f for three different values of pump signal power: $P_{pump} < P_{cr}$(a); $P_{pump} \simeq P_{cr}$ (b); $P_{pump} \geq P_{cr}$ (c). The frequency of the pump signal was 7.74328 GHz. The externally applied magnetic field is zero. Note the weaker mirror idler resonance at 7.741145 GHz in panels (a) and (b), as indicated by red arrows, corresponding to the idler mode of the Bogoliubov excitations.

In Fig. 3(a) we present experimentally observed dependencies of the resonance (dip) frequency on the pump power P_{pump} for several pump frequencies f_{pump}. The

dip position exhibits a pronounced dependence on f_{pump}, and the sharp frequency drop was observed within a narrow pump-frequency window, 7.743 GHz $< f_{pump} <$ 7.746 GHz, only. In addition, as f_{pump} is increased slightly within this range, the magnitude of the drop decreases and the threshold pump power P_{cr} shifts to lower values (see, red, black and green curves in Fig. 3a). As the pump frequency is outside this narrow window, a sharp frequency drop was not observed, and a smooth dependence of the dip frequency position on the pump power of P_{pump} was obtained.

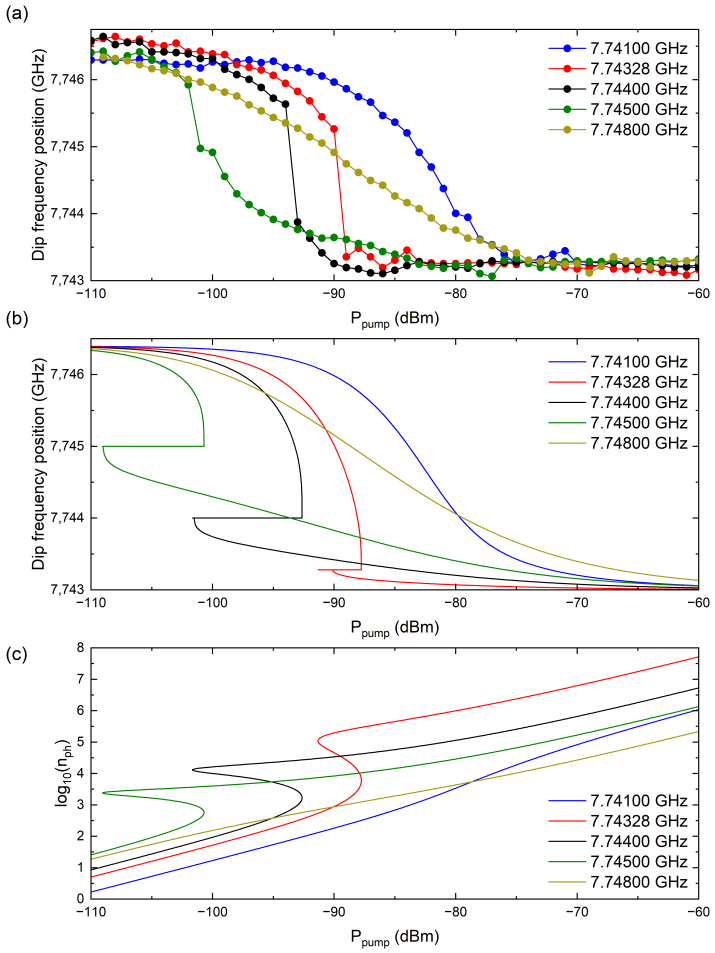


Figure 3: (a) The experimental dependence of the dip frequency position on the pump power P_{pump} for different frequencies of the pump signal.(b) Calculated dependencies of the dip frequency position on the pump power P_{pump} for different frequencies of the pump signal. (c) Deduced photon number inside the cavity. To obtain the best fit to the experimental curves we choose the following parameters as: $\omega_c = 2\pi \times 7.7430 GHz$, $\gamma = 2\pi \times 3.2 MHz$, $\Delta = 2\pi \times 1.78\, GHz$ and the coupling strength of a single qubit to the R-resonator, $g = 2\pi \times 25\, MHz$.

Within this pump frequencies window, i.e., 7.743 GHz $< f_{pump} <$ 7.746 GHz,

several observations are consistent with the presence of a *bistable response* of the microwave photon field. First, the frequency position of the resonant dip does not shift smoothly with pump power, but exhibits an abrupt jump as P_{pump} is swept from –110 dBm to –60 dBm (see Fig. 3). Second, the $|S_{21}|$ spectra shown in Fig. 2 reveal the appearance of a secondary dip as P_{pump} approaches the threshold value P_{cr} (Fig. 2b). For $P_{pump} \geq P_{cr}$, this secondary dip becomes the dominant spectral signature (Fig. 2c), indicating a switch to an alternative metastable state. Further evidence for bistability is provided by the small hysteresis observed in Fig. 4: near P_{cr}, the resonance frequency depends on the direction of the pump-power sweep, forming a hysteretic loop when P_{pump} is ramped up and subsequently ramped down over the same range.

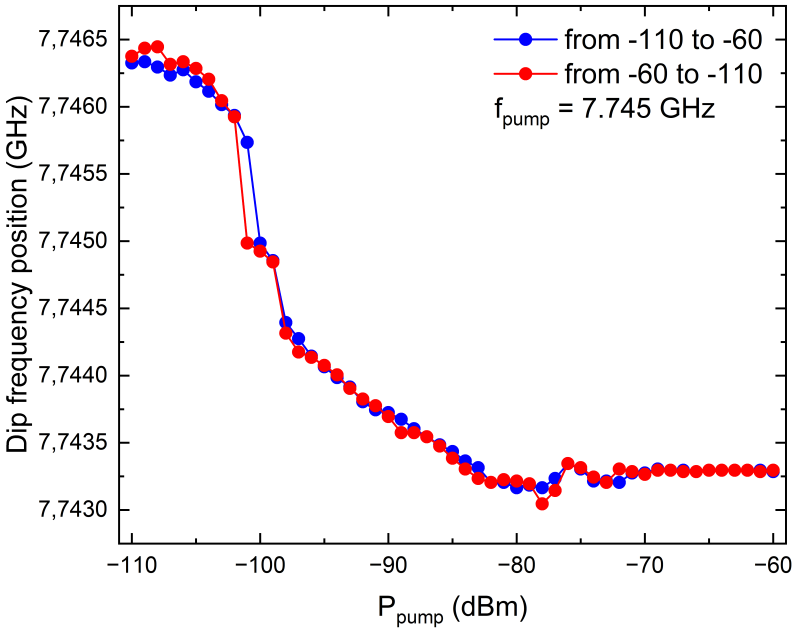


Figure 4: The dependence of the dip frequency position on the pump signal power P_{pump} for different directions of power sweep. The frequency of a pump signal was 7.745 GHz

We also performed the two-tone spectroscopy measurements in hysteresis regime (f_{pump}=7.74328 GHz) under a static magnetic field $B = 0.489\ G$. The results presented in Fig. 5 report a shift of the pump power threshold P_{cr} to lower values as a static magnetic field was applied. This decreasing of the threshold power can be described by the changing of the SQN qubit frequencies induced by the magnetic field, which, in turn, modifies the energy required by the pump photons to induce a nonlinear response.

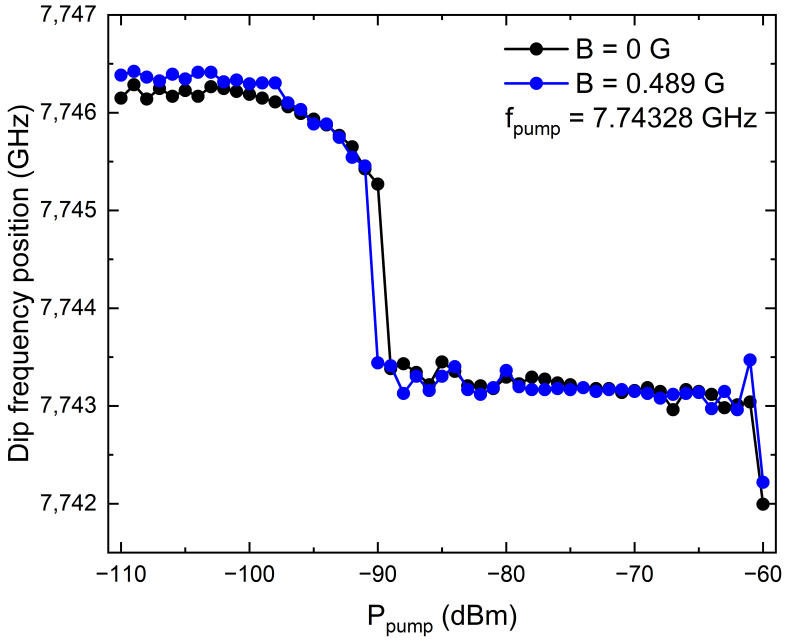


Figure 5: The dependence of the dip frequency position on the pump power in the presence of a static magnetic field, $B = 0.489G$, The pump frequency was f_{pump}=7.74328 GHz.

Theory: Collective Bogoliubov modes of Microwave Photons

General analysis: We model the complete system as an SQN composed of N qubits coupled to high quality R and T resonators. Each qubit is characterized by a qubit frequency, ω_j, and both T- and R resonators have an identical resonance frequency ω_c. Such system is described by a time-dependent nonlinear Gross-Pitaevskii-like equation for the photon field inside the R+T-resonator, $\psi(t)$, written in the system rotating with the pump frequency ω_0 and normalized such that the average photon number is $n_{ph} = |\psi(t)|^2$. In the presence of an externally applied microwave input signal, $x_{in}(t)$, the dynamic equation for the photon field $\psi(t)$ is written as (see the

derivation of Eq. (1) in Methods, parts B and C).

$$\left[i\frac{d}{dt} + \omega_0 - \omega_c - \sum_{j=1}^{N} \frac{g_j^2/\Delta_j}{\sqrt{1+4g_j^2|\psi(t)|^2/\Delta_j^2}} + i\frac{\gamma}{2} \right] \psi(t) = \sqrt{\frac{\omega_c}{2|Q_c|}} \frac{x_{in}(t)}{i}, \qquad (1)$$

where $\omega_0 = 2\pi f_{pump}$ is the pump frequency; $\Delta_j = \omega_0 - \omega_j$, and g_j is the coupling of the j-th qubit to the R-resonator. We also introduce the R-resonator dissipation, $\gamma = \omega_0/Q_l$, where Q_l is the loaded quality factor of the R resonator (see Methods, parts C and D). The interaction between photons is produced by the Stark shift of qubits frequencies induced by the coupling between an SQN and microwave photons. This interaction results in a specific non-linearity of Eq. (1) quite different from the one occurring in the Gross-Pitaevskii equation [2], disappearing in the limit of a strong photon field (a large number of photons), and therefore, restraining the nonlinear effects to a delimited range of power.

As only one external microwave signal, i.e., the microwave pump tone, is applied, the input is a stationary one, $x_{in}(t) = x_0$, where x_0 is determined by the pump power as $|x_0|^2 = P_{pump}/\hbar\omega_c$. In this case we obtain the stationary solution of Eq. (1) and determine the total photon number inside the resonator, n_{ph}, as a solution of the transcendent equation

$$n_{ph} = \frac{2P_{pump}/(\hbar|Q_c|)}{\gamma^2 + 4[\omega_0 - \omega_r(n_{ph})]^2}, \qquad (2)$$

where we define the photon number dependent resonance frequency $\omega_r(n_{ph})$ as

$$\omega_r(n_{ph}) = \omega_c + \sum_{j=1}^{N} \frac{g_j^2/\Delta_j}{\sqrt{1+4g_j^2 n_{ph}/\Delta_j^2}}. \qquad (3)$$

Here, Q_c is an external coupling quality factor. Notice here, that the frequency $\omega_r(n_{ph})$

determines the microwave power dependent frequency position of the narrow resonant drop in a *single tone* spectroscopy measurements, i.e., the dependence $|S_{33}(\omega_0)|$ presented in Eq.(S1) of the Supplementary Material.

Bogoliubov-like collective excitations: In two-tone spectroscopy measurements where both a strong pump and a weak probe microwave fields are present, one can take an external microwave input in the following form: $x_{in}(t) = x_0 + a\exp[-i(\omega - \omega_0)t]$ with a small signal amplitude, $|a| \ll |x_0|$. Here, $\omega = 2\pi f$ is the frequency of a weak microwave probe. The corresponding time-dependent solution of Eq. (1) is written as $\psi(t) = \sqrt{n_{ph}} + e^{-i(\omega-\omega_0)t}u + e^{i(\omega-\omega_0)t}v$.

In this case the solution of Eq. (1) determines the eigenfrequency $\tilde{\omega}(n_{ph})$ of the Bogoliubov-like collective excitations induced by a weak probe microwave field:

$$\tilde{\omega}(n_{ph}) = \omega_0 - [\omega_0 - \omega_r(n_{ph})]\mathrm{Re}\sqrt{1 + \sum_{j=1}^{N} \frac{4g_j^4 n_{ph}}{[\omega_0 - \omega_r(n_{ph})](\Delta_j^2 + 4g_j^2 n_{ph})^{3/2}}}, \qquad (4)$$

where $\tilde{\omega}(n_{ph})$ determines implicitly the dependence of the frequency position of the resonant drop on the microwave pump power P_{pump} in the $|S_{21}|$ measurements. These collective excitations correspond to the Bogoliubov modes occurring in a system of interacting photons collected in the R-resonator.

We also notice that the oscillating photon field in addition to the probe frequency ω contains also the idler mode of the frequency, $2\omega_0 - \omega$. This idler wave is analogous to the one used in quantum optics [49] or microwave optics [50] in the context of parametric amplifiers for generating quantum entanglement of continuous variables. This idler mode should be visible and it provides another justification of the Bogoliubov approach. Indeed, such idler resonances can be seen in the experimental resonant curves reported in Fig. 2(a) and (b), and it was highlighted by red arrows.

Bistability: The nonlinear dependence of the total number of photons on the microwave pump power (see, Eqs. (2) and (3)) can result in multiple solutions, e.g., in bistability. Bistability is triggered once both conditions $dP_{pump}/dn_{ph} =$

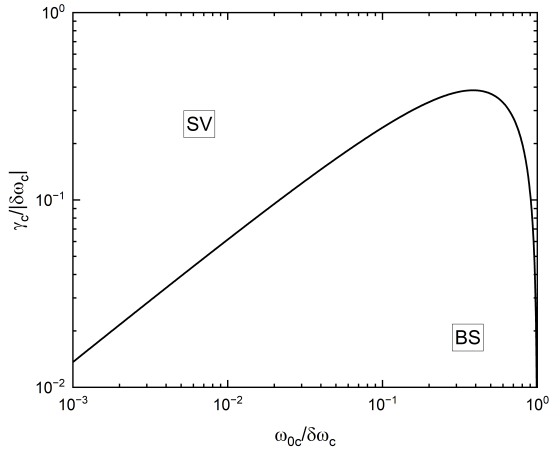


Figure 6: Phase diagram $\gamma/(\delta\omega_c) - -\omega_{0c}/(\delta\omega_c)$ delimiting the single value (SV) region from the bistability region (BS).

$d^2P_{pump}/dn_{ph}^2 = 0$ are fulfilled in Eq.(2). Assuming equal detunings $\Delta_j = \Delta$ and coupling constants for the qubits $g_j = g$, we determine the range of system parameters where two stable values of a photon number n_{ph} can coexist for a fixed microwave pump power. Defining the detuning of the pump tone, $\omega_{0c} = \omega_0 - \omega_c$, and the resonator frequency shift, $\delta\omega_c = Ng^2/\Delta$, introducing the dimensionless parameter $s = 1 + 4g^2 n_{ph}/\Delta^2$ and using both conditions, we obtain the following bounds:

$$\frac{\gamma}{|\omega_{0c}|} < \frac{\sqrt{3}}{2}\frac{s^2-1}{s} \qquad \left|\frac{\delta\omega_c}{\omega_{0c}}\right| > \frac{3s+s^3}{4} \tag{5}$$

The elimination of the variable s in the expressions (5) leads to a line $\gamma - \omega_{0c}$ separating the single- and bistability regions and shown in Fig. 6. Thus, the bistabilty of microwave photon field can be observed as the pump detuning does not exceed the resonator frequency shift, i.e., $\omega_{0c} < \delta\omega_c$, and the losses are low. The optimal conditions are determined by the maximum of the separation line (see, Fig. 6), i.e., $\gamma = |\omega_{0c}| = 2|\delta\omega_c|/(3\sqrt{3})$. Typical curves of $n_{ph}(P_{pump})$ indicating the bistable behavior are presented in Fig. 3c.

Discussion

The Eqs.(2)-(4) form a self consistent set to quantitatively describe the coherent collective states in the microwave photon field trapped in the resonator. This analysis demonstrates that in the regime of a low pump power as the number of trapped photons $n_{ph} \ll \Delta^2/g^2$ the Bogoliubov mode frequency $\tilde{\omega}$ shifts to $\tilde{\omega} = \omega_c + \delta\omega_c$, where $\delta\omega_c = \sum_{j=1}^{N} \frac{g_j^2}{\Delta_j}$, and in the opposite regime of a large pump power as $n_{ph} \gg \Delta^2/g^2$, the $\tilde{\omega}$ tends to the value $\tilde{\omega} \simeq \omega_c$. . Thus, one can expect the bistable regions in the dependence of the frequency of Bogoliubov modes on the pump power as the pump frequency falls in the narrow window, $\omega_c < \omega_0 < \omega_c + \delta\omega_c$.

The numerically calculated dependencies of the Bogoliubov mode frequencies on the pump tone power, P_{pump}, are presented in Fig. 3(b). The calculations were performed by using Eq. (4) and taking into account the experimental results shown in Fig. 3a. Assuming equal coupling $g_j = g$ and equal qubit detuning $\Delta_j = \Delta$, the quantitative fit of the six experimental curves shown in Fig.(3) with Eq.(4) allows to obtain the frequency shift $\delta\omega_c = Ng^2/\Delta = 2\pi \times 3.4MHz$ and extract the two remaining parameters g, Δ using $N = 10$. Note that the deduced quality factor $Q_c \simeq$ 25000 corresponds rather to the coupling quality factor Q_c extracted from the fit of S_{33} (see Methods, section D). The difference with Q_c can be explained by an additional fluorescence from a strong pump causing an additional leakage (which will be the topic of a subsequent work). Comparing the Figs. 3a and b we obtain a good quantitative agreement between theoretical calculations and the experimental data. Assuming that the magnetic field B acts only on the qubit frequencies, we estimate from Fig.(5) at low power the shift variation: $d\omega_r/dB \simeq 0.2MHz/0.489G$. From Eq.(3), we deduce the qubit frequency shift per Gauss: $d\omega_j/dB \simeq (\Delta/\delta\omega_c)(d\omega_r/dB) \sim 200MHz/G$ in agreement with expectations. The visible dependence of critical pump power on magnetic field remains difficult to interpret as we did not observe significant change of the bistability region by tuning the qubit frequency.

We also note a plateau region where $\tilde{\omega} = \omega_0$ and the square root in Eq.(4) becomes imaginary. A similar theoretical approach has been applied in [36] for describing the instability phenomenon experimentally observed on a SQUID metamaterial in nonlinear regime reported in [35].

Conclusion and future perspectives

In conclusion, in this work we present, for the first time to our knowledge, the experimental evidences of a Bose-Einstein like condensate of microwave photons in the strongly driven resonator mode and the emergence of Bogoliubov excitations above this macroscopically occupied state. In detail, we proposed, fabricated and tested a quantum device in which two low-dissipative superconducting resonators coupled through an embedded superconducting qubits network (SQN). The frequency position of the narrow resonant dip observed in the frequency dependent transmission coefficient of a small probe signal, demonstrates an abrupt *red shift* once the pump power exceeds a critical threshold. This transition occurs within a narrow range of pump frequencies, indicating a well-defined dynamical regime where the collective photon–qubit interactions dominate the system response.

The observed bistable and hysteretic response is quantitatively described by a model in which the nonlinear multiphoton interaction mediated by the qubit ensemble, occurs. In this model the experimental findings obtain natural explanation as the fingerprint of collective Bogoliubov excitations in a Bose-Einstein like condensate of microwave photons.

Beyond providing experimental evidence of these collective states, our results highlight the potential of superconducting qubit networks as nonlinear quantum media in which photon interactions can be engineered and controlled. The pronounced bistability and hysteresis observed in the transmission response suggest possible applications

in circuit quantum electrodynamics architectures, including threshold microwave detectors, quantum-limited sensing schemes, and bistable memory elements.

More broadly, the demonstrated platform provides a promising route to explore driven many-body photonic phenomena in superconducting resonant circuits, while also pointing to the possibility that suitably engineered qubit-network topologies could stabilize and enhance collective responses, opening the way to topologically informed sensing architectures and in-sensor quantum information processing. In particular, both theoretical and experimental work is in progress to understand if "cross-type" geometrical configurations of the qubits in a SQN embedded in a two resonators microwave device can contribute to the enhancement of both transport properties (in direct current regime) and susceptivity as function of the frequency due to topological effects as predicted by our papers [51, 52].

Methods

A. Device Fabrication

The fabrication of T- and R- resonators was performed by patterning a Nb film deposited on a silicon substrate. The flux qubits were realized in Al by two-angle shadow evaporation technique, forming three Josephson junctions loops, each one incorporating two identical junctions, while the third one is scaled of a factor 0.8. Additional details on the fabrication process and on the flux qubit parameters are reported in Supplementary Materials.

B. Experimental setup

For scattering-parameter measurements, the SQN network was mounted on a dedicated sample holder and cooled down in a Leiden Cryogenics CF-CS110-1000 dilu-

tion refrigerator installed at Laboratori Nazionali di Frascati (Italy). A static magnetic field was generated by a superconducting NbTi filament wound around the holder, while microwave excitation was provided through one of the RF input lines. The transmission spectra of the T- and R-resonators were acquired using an Agilent E5071C Vector Network Analyzer (VNA). Further details on the experimental setup scheme are reported in Supplementary Material.

C. Derivation of cavity field equation

C.1. Basic equations

Our approach relies on the formalism for a cavity derived in [53], with the main difference that, as the result of mutual coupling, we consider the two cavity R+T as one effective resonator of frequency ω_c. At port 3, the input electromagnetic field in a waveguide in the z direction with the coordinate r_z can be represented by the forward + and backward − microwave fields

$$A_{\pm}(r_z,t) \;=\; \frac{V(r_z,t) \pm ZI(r_z,t)}{2\sqrt{Z}}. \tag{6}$$

These are the classical voltage and current usually associated to a coplanar waveguide. Z is the impedance of the line (and usually fixed to $60Hz$ for quantum circuit). The input field is a free propagating field while the scattered one results from the interaction with the resonator and the qubits. Around the pump frequency ω_0 viewed also as a carrier frequency, we rewrite quite generally the field envelop caused by an amplitude modulation (or frequency modulation on convenience) at the cavity end $r_z = 0$ on port 3 :

$$A_{-}(0,t) = \sqrt{2\hbar\omega_c}\mathrm{Re}(x_{out}(t)e^{-i\omega_0 t}) \tag{7}$$

$$A_{+}(0,t) = \sqrt{2\hbar\omega_c}\mathrm{Re}(x_{in}(t)e^{-i\omega_0 t})\,. \tag{8}$$

The qubits are placed inside the cavity end for a maximum coupling to the field.

Adding the dephasing $\Gamma_{\phi,j}$ due to Josephson junction and the decay rate Γ_j to a transverse channel (due to other cavity modes), we obtain the master equation for the matrix density $\hat{\rho}(t)$ [53]:

$$\begin{aligned} & \partial_t\hat{\rho}(t) + i[\hat{H}_S(t), \hat{\rho}(t)] \\ = \; & \frac{\gamma}{2}\left[2\hat{a}\hat{\rho}(t)\hat{a}^\dagger - \{\hat{a}^\dagger\hat{a}, \hat{\rho}(t)\}\right] - \sum_{j=1}^{N}(\frac{\Gamma_j}{2} + \Gamma_{\phi,j})\{\hat{\sigma}_j^+\hat{\sigma}_j^-, \hat{\rho}(t)\} - \Gamma_j\hat{\sigma}_j^-\hat{\rho}(t)\hat{\sigma}_j^+ \, . \end{aligned} \tag{9}$$

where $[.,.]$ and $\{.,.\}$ are the commutator and the anticommutator respectively. The associated system Hamiltonian written in the rotating wave approximation (RWA) is:

$$\begin{aligned} \hat{H}_S(t) \; = \; & -\omega_{0c}\hat{a}^\dagger\hat{a} + i\sqrt{\frac{\omega_c}{2|Q_c|}}(x_{in}^*(t)\hat{a} - x_{in}(t)\hat{a}^\dagger) \\ - \; & \sum_{j=1}^{N}\left[\frac{\Delta_j}{2}\hat{\sigma}_j^z + g_j(\hat{a}^\dagger\hat{\sigma}_j^- + \hat{a}\hat{\sigma}_j^+)\right] , \end{aligned} \tag{10}$$

where we define the Pauli matrices, describing the jth qubit, $\hat{\sigma}_j^{x,y,z}$, and the Bose operators $\hat{a}^\dagger, \hat{a}$. The lifetime $T_{ph} = 1/\gamma = Q_l/\omega_c$ for the photon within the T+ R-resonator is expressed in terms of the load quality factor Q_l with the decomposition:

$$\frac{1}{Q_l} = \left|\frac{1}{Q_c}\right| + \frac{1}{Q_i} \tag{11}$$

which includes also the internal losses Q_i, mainly fluorescence, in the relaxation rate of photon leakage in (9) and differs from [53] where $Q_i \to \infty$. Note that for the second tone of weak intensity, the internal loss is negligible and therefore $Q_l \simeq Q_c$.

This lifetime is assumed to be much shorter to the relaxation times for decay $T_{1,j} = 1/\Gamma_j$ and for pure dephasing $T_{2,j} = 1/\Gamma_{\phi,j}$ since, due to the Purcell effect, the qubits interact mainly with the cavity field mode. Their relaxation rates will be therefore neglected in the following compared to the leakage rate γ.

The master equation (9) describes only the dynamics of qubit due to an external field. However, we need to specify another relation with the scattered field generated

from the qubit evolution. For this purpose, we use the Fourier transform in time of the field as [53]:

$$A_{\pm}(r_z,t)=\int_{-\infty}^{\infty}\frac{d\omega}{2\pi}e^{-i(\omega+i\eta)t}A_{\omega,\pm}(r_z) \tag{12}$$

where we have introduced the positive and infinitesimal parameter $\eta\to 0$ to ensure an adiabatic switching essential to study the retarded response to any input wave.

Restricting the frequency domain close to the cavity mode, the reflection is (up to a prefactor neglected here):

$$S_{33}=\frac{A_{\omega_0,-}(0)}{A_{\omega_0,+}(0)}=1-\sum_{\pm}\frac{e^{i\phi}Q_l\gamma/2}{\omega_0-(\pm\omega_c-i\gamma_c/2)}\left[\frac{i}{|Q_c|}\pm\sqrt{\frac{\hbar}{|Q_c|}}\sum_{j=1}^{N}\frac{g_j\langle\hat{\sigma}^{\mp}_{\omega_0,j}\rangle}{A_{\omega_0,+}(0)}\right] \tag{13}$$

where we use a similar definition to (12) for the Fourier transform $\hat{\sigma}^{\mp}_{\omega_0,j}$ in the undressed representation. We include phenomenologically the internal loss with finite internal quality factor and the mismatch phase factor ϕ [54], in contrast to [53] where we use $\phi=0$.

C.2. Semi-classical solution

Using the Glauber-Sudershan transformation $\hat{D}(t)$, we rewrite the cavity field as:

$$\hat{a}\to\hat{D}^{\dagger}(t)\hat{a}\hat{D}(t)=\hat{a}+\psi(t) \tag{14}$$

where $\psi(t)$ is the coherent field inside the resonator while the new $\hat{a}$ defines now the quantum fluctuations operator. Similarly we can redefine the qubit operators adequately in the dressed state representation. Using the polar decomposition $\psi(t)=e^{i\theta(t)}\sqrt{n_{ph}(t)}$ we define

$$\hat{\sigma}^{x}_{j}=e^{-i\theta(t)}\hat{\sigma}^{-}_{j}+e^{i\theta(t)}\hat{\sigma}^{+}_{j} \tag{15}$$

$$\hat{\sigma}^{y}_{j}=i(e^{-i\theta(t)}\hat{\sigma}^{-}_{j}-e^{i\theta(t)}\hat{\sigma}^{+}_{j}) \tag{16}$$

and, after an additional rotation about the y-axis in the qubit Bloch sphere, we use the new basis:

$$\hat{\sigma}_j'^z = \cos\theta_j(t)\hat{\sigma}_j^z + \sin\theta_j(t)\hat{\sigma}_j^x \tag{17}$$

$$\hat{\sigma}_j'^x = -\sin\theta_j(t)\hat{\sigma}_j^z + \cos\theta_j(t)\hat{\sigma}_j^x \tag{18}$$

$$\cos\theta_j(t) = \frac{|\Delta_j|}{\sqrt{\epsilon_j^2(t)+\Delta_j^2}} \qquad \sin\theta_j(t) = \frac{\Delta_j\epsilon_j(t)/|\Delta_j|}{\sqrt{\epsilon_j^2(t)+\Delta_j^2}} \tag{19}$$

where $\epsilon_j(t) = 2g_j|\psi(t)|$ is the Rabi frequency of qubits j. Using these successive time-dependent unitary transformations, the Hamiltonian has the new form (omitting the time dependence notation):

$$\begin{aligned}\hat{H}_S' = &\left[\left(i\frac{d}{dt} + \omega_{0c} - \sum_{j=1}^{N}\frac{g_j^2/\Delta_j}{\sqrt{1+\epsilon_j^2/\Delta_j^2}}\right)\psi\hat{a}^\dagger + i\sqrt{\frac{\omega_c}{2|Q_c|}}x_{in}\hat{a}^\dagger + c.c.\right] \\ - &\sum_{j=1}^{N}\left[\frac{\sqrt{1+\epsilon_j^2/\Delta_j^2}}{2}\Delta_j(\hat{\sigma}_j'^z+1) + \frac{g_j(\epsilon_j(\hat{\sigma}_j'^z+1)+\Delta_j\hat{\sigma}_j'^x)}{2\Delta_j\sqrt{1+\epsilon_j^2/\Delta_j^2}}(e^{-i\theta}\hat{a}+e^{i\theta}\hat{a}^\dagger)\right. \\ + &\left.\frac{ig_j}{2}\hat{\sigma}_j^y(e^{-i\theta}\hat{a}-e^{i\theta}\hat{a}^\dagger)\right] + \mathcal{F}(\psi,\psi^*)\end{aligned} \tag{20}$$

where we define the Landau-Ginzburg-like function

$$\begin{aligned}\mathcal{F}(\psi,\psi^*) = &\frac{i}{2}\left(\frac{d\psi^*}{dt}\psi - \frac{d\psi}{dt}\psi^*\right) - \omega_{0c}|\psi|^2 + \frac{1}{2}\sum_{j=1}^{N}\Delta_j\sqrt{1+4g_j^2|\psi|^2/\Delta_j^2} \\ + &\; i\sqrt{\frac{\omega_c}{2|Q_c|}}(x_{in}^*\psi - x_{in}\psi^*)\,,\end{aligned} \tag{21}$$

In absence of cavity leakage, the latter corresponds to a Lagrangian allowing alternatively to recover the dynamic equation (1). It is an analog of the Gross-Pitaevski equation but with a different form for the non-linearity. To obtain (20), we have neglected the derivative terms $d\theta/dt$ and $d\theta_j/dt$ resulting from the time dependent

unitary transformation as they are assumed small ($\sim 2\pi$ MHz) in comparison to the detuning Δ_j ($\sim 2\pi 100$ MHz). These transformations redefine the density matrix $\hat{\rho}$ into $\hat{\rho}'$ as well as the master equation which becomes:

$$\partial_t \hat{\rho}' + i[\hat{H}'_S, \hat{\rho}'] = \frac{\gamma_c}{2}\left[2(\hat{a}+\psi)\hat{\rho}'(\hat{a}^\dagger+\psi^*) - \{(\hat{a}^\dagger+\psi^*)(\hat{a}+\psi), \hat{\rho}'\}\right] . \quad (22)$$

We cancel out all the linear terms in the creation annihilation operator in Eq.(22) by imposing the condition of Eq.(1). The remaining contributions are negligible in the semi-classical approximation when the coherent field is important ($|\psi|^2 \gg 1$) in comparison to quantum fluctuations. Therefore we omit the quantum part of the cavity photon field in the interaction with the qubits and the master equation reduces more simply to:

$$\partial_t \hat{\rho}' - i[\omega_{0c}\hat{a}^\dagger\hat{a} + \sum_{j=1}^{N} \frac{\sqrt{1+\epsilon_j^2/\Delta_j^2}}{2}\Delta_j(\hat{\sigma}_j'^z + 1), \hat{\rho}'] = \frac{\gamma_c}{2}\left[2\hat{a}\hat{\rho}'\hat{a}^\dagger - \{\hat{a}^\dagger\hat{a}, \hat{\rho}'\}\right] . \quad (23)$$

It has the trivial ground state solution where $\langle \hat{a}^\dagger\hat{a}\rangle = 0$ and $\langle \hat{\sigma}_j'^z\rangle = -1$. Returning to the initial representation, we deduce:

$$\langle \hat{\sigma}_j^- \rangle = -\frac{2g_j\psi/\Delta_j}{\sqrt{1+4g_j^2 n_{ph}/\Delta_j^2}} \quad (24)$$

Therefore the dynamics is mainly governed by Eq.(1) in the semi-classical case. In the case of the steady state solution where $x_{in} = x_0$ is time-independent, we find

$$\psi = \frac{-ix_0\sqrt{\omega_c/2|Q_c|}}{\omega_s + i\gamma_c/2} \quad (25)$$

If we apply the Fourier transform defined in Eq.(12) to Eq.(7) and to Eq.(24) combined with Eq.(25) written in the undressed representation and, second, we insert the results into Eq.(13) and use the rotating wave approximation, we obtain the Eq.(S1) for S_{33} reported in Supplementary Material.

D. Loss parameter estimation of R- resonator

The estimation of loss parameters, i.e., the loaded quality factor Q_l and the coupling quality factor, Q_c, was carried out by fitting of S_{33} resonant experimental curve measured by a single tone spectroscopy of R-resonator. This process allowed us to estimate the parameters $Q_c = 24530.93 \pm 0.38$ and $Q_l = 4682.71 \pm 0.05$. Further details on this estimation are provided in the Supplementary Material.

References

[1] L. D. Landau and E. M. Lifsits. *Statistical Physics, vol. 9.* Oxford, 1980.

[2] L. P. Pitaevskii and S. Stringari. *Bose–Einstein Condensation and Superfluidity*, volume 164 of *International Series of Monographs on Physics*. Oxford University Press, 2016.

[3] N. P Proukakis. A century of bose-einstein condensation. *Communications Physics*, 8(1):264, 2025.

[4] M. H. Anderson, J. R. Ensher, M. R. Matthews, C. E. Wieman, and E. A. Cornell. Observation of bose-einstein condensation in a dilute atomic vapor. *science*, 269(5221):198–201, 1995.

[5] J. R. Anglin and W. Ketterle. Bose–einstein condensation of atomic gases. *Nature*, 416(6877):211–218, 2002.

[6] G. Roati, C. D'Errico, L. Fallani, M. Fattori, C. Fort, M. Zaccanti, G. Modugno, M. Modugno, and M. Inguscio. Anderson localization of a non-interacting bose–einstein condensate. *Nature*, 453(7197):895–898, 2008.

[7] J. E. Lye, L. Fallani, M. Modugno, D. S. Wiersma, C. Fort, and M. Inguscio. Bose-einstein condensate in a random potential. *Physical review letters*, 95(7):070401, 2005.

[8] Y. Nakagawa, Y. Kasahara, T. Nomoto, R. Arita, T. Nojima, and Y. Iwasa. Gate-controlled bcs-bec crossover in a two-dimensional superconductor. *Science*, 372(6538):190–195, 2021.

[9] Q. Chen, Z. Wang, R. Boyack, S. Yang, and K. Levin. When superconductivity crosses over: From bcs to bec. *Reviews of Modern Physics*, 96(2):025002, 2024.

[10] S. O. Demokritov, V. E. Demidov, O. Dzyapko, G. A Melkov, A. A. Serga, B. Hillebrands, and A. N. Slavin. Bose–einstein condensation of quasi-equilibrium magnons at room temperature under pumping. *Nature*, 443(7110):430–433, 2006.

[11] A. A. Serga, V. S. Tiberkevich, C. W. Sandweg, V. I. Vasyuchka, D. A. Bozhko, A. V. Chumak, T. Neumann, B. Obry, G. A. Melkov, A. N. Slavin, et al. Bose–einstein condensation in an ultra-hot gas of pumped magnons. *Nature communications*, 5(1):3452, 2014.

[12] H. Deng, H. Haug, and Y. Yamamoto. Exciton-polariton bose-einstein condensation. *Reviews of modern physics*, 82(2):1489–1537, 2010.

[13] J. Kasprzak, M. Richard, S. Kundermann, A. Baas, P. Jeambrun, J. M. J. Keeling, F. M. Marchetti, M. H. Szymańska, R. André, J. L. Staehli, et al. Bose–einstein condensation of exciton polaritons. *Nature*, 443(7110):409–414, 2006.

[14] J. Klaers, J. Schmitt, F. Vewinger, and M. Weitz. Bose–einstein condensation of photons in an optical microcavity. *Nature*, 468(7323):545–548, 2010.

[15] Y. Wu, S. B. Bao, S. Cao, F. Chen, M. C Chen, X. Chen, T. H. Chung, H. Deng, and Y. et al Du. Strong quantum computational advantage using a superconducting quantum processor. *Physical Review Letters*, 127:180501, 2021.

[16] A. J. Leggett, B. Ruggiero, and P. Silvestrini. *Quantum computing and quantum bits in mesoscopic systems*. Springer, 2004.

[17] R Ozeri, N Katz, J Steinhauer, and N Davidson. Colloquium: bulk bogoliubov excitations in a bose-einstein condensate. *Reviews of Modern Physics*, 77(1):187–205, 2005.

[18] R. Y. Chiao. Bogoliubov dispersion relation for aphoton fluid': Is this a superfluid? *Optics communications*, 179(1-6):157–166, 2000.

[19] A. Wallraff, D. I. Schuster, A. Blais, L. Frunzio, R. S. Huang, J. Majer, S. Kumar, S. M. Girvin, and R. J. Schoelkopf. Strong coupling of a single photon to a superconducting qubit using circuit quantum electrodynamics. *Nature*, 431(7005):162–167, 2004.

[20] A. Blais, A. L. Grimsmo, S. M. Girvin, and A. Wallraff. Circuit quantum electrodynamics. *Reviews of Modern Physics*, 93(2):025005, 2021.

[21] D. I. Schuster, A. A. Houck, J. A. Schreier, A. Wallraff, J. M. Gaambetta, A. Blais, L. Frunzio, J. Majer, B. Johnson, M. H. Devoret, S. M. Girvin, and R. J. Schoelkopf. Resolving photon number states in a superconducting circuit. *Nature*, 445:515, 2007.

[22] P. Macha, G. Oelsner, J. M. Reiner, M. Marthaler, S. André, G. Schön, U. Hübner, H. G. Meyer, E. Il'ichev, and A. V. Ustinov. Implementation of a quantum metamaterial using superconducting qubits. *Nature communications*, 5(1):5146, 2014.

[23] K. V. Shulga, P. Yang, G. P. Fedorov, M. V. Fistul, M. Weides, and A. V. Ustinov. Observation of a collective mode of an array of transmon qubits. *JETP letters*, 105(1):47–50, 2017.

[24] J. D. Brehm, A. N. Poddubny, A. Stehli, T. Wolz, H. Rotzinger, and A. V. Ustinov. Waveguide bandgap engineering with an array of superconducting qubits. *npj Quantum Materials*, 6:10, 2021.

[25] P. Krantz, M. Kjaergaard, F. Yan, T. P. Orlando, S. Gustavsson, and W. D. Oliver. A quantum engineer's guide to superconducting qubits. *Applied Physics Reviews*, 6:021318, 2019.

[26] M. Kjaergaard, M. E. Schwartz, J. Braumüller, P. Krantz, J. I.-J. Wang, S. Gustavsson, and W. D. Oliver. Superconducting qubits: Current state of play. *Annual Review of Condensed Matter Physics*, 11:369, 2020.

[27] M. Boissonneault, J. M. Gambetta, and A. Blais. Improved superconducting qubit readout by qubit-induced nonlinearities. *Physical Review Letters*, 105:100504, 2010.

[28] M. V. Fistul, O. Neyenhuys, A. B. Bocaz, M. Lisitskiy, and I. M. Eremin. Quantum dynamics of disordered arrays of interacting superconducting qubits: Signatures of quantum collective states. *Physical Review B*, 105:104516, 2022.

[29] P. Macha, G. Oelsner, J.-M. Reiner, M. Marthaler, St. André, G. Schön, U. Hübner, H.-G. Meyer, E. Il'ichev, and A. V. Ustinov. Implementation of a quantum metamaterial using superconducting qubits. *Nature Communications*, 5:5146, 2014.

[30] K. V. Shulga, P. Yang, G. P. Fedorov, M. V. Fistul, M. Weides, and A. V. Ustinov. Observation of a collective mode of an array of transmon qubits. *JETP Letters*, 105:47, 2017.

[31] Sh. Puri, S. Boutin, and A. Blais. Engineering the quantum states of light in a kerr-nonlinear resonator by two-photon driving. *npj Quantum Information*, 3:18, 2017.

[32] N. Maleeva, L. Grünhaupt, T. Klein, F. Levy-Bertrand, O. Dupre, M. Calvo, et al. Circuit quantum electrodynamics of granular aluminum resonators. *Nature Communications*, 9:3889, 2018.

[33] E. Enrico, C. Bonavolontà, G. Brida, G Coda, E Il'Ichev, L. Fasolo, M. Fistoul, A. Meda, L. Oberto, G. Oelsner, et al. Superconducting qubit network as a single microwave photon detector for galactic axion search. *IEEE Transactions on Applied Superconductivity*, 34(3):1–6, 2023.

[34] C. Gatti, M. Affronte, A. Balanov, C. Bonizzoni, G. Brida, F. Chiariello, N. Chikhi, G. Coda, A. D'Elia, D. Di Gioacchino, et al. Coherent quantum network of superconducting qubits as a highly sensitive detector of microwave photons for searching of galactic axions. *IEEE Transactions on Applied Superconductivity*, 33(5):1–5, 2023.

[35] P. Jung, S. Butz, M. Marthaler, M. V. Fistul, Ju. Leppäkangas, V. P. Koshelets, and A. V. Ustinov. Multistability and switching in a superconducting metamaterial. *Nature Communications*, 5:3730, 2014.

[36] E. I. Kiselev, A. S. Averkin, M. V. Fistul, V. P. Koshelets, and A. V. Ustinov. Two-tone spectroscopy of a squid metamaterial in the nonlinear regime. *Physical Review Research*, 1:033096, 2019.

[37] Oded Yaakobi, Lazar Friedland, Chris Macklin, and Irfan Siddiqi. Parametric amplification in josephson junction embedded transmission lines. *Physical Review B—Condensed Matter and Materials Physics*, 87(14):144301, 2013.

[38] AS Averkin, AA Kopasov, IE Pologov, Aleksey N Bolgar, Daria A Kalacheva, Viktor B Lubsanov, MV Fistul, and A Karpov. Strongly nonlinear regime of josephson transmission lines revealed by two-tone spectroscopy. *Physical Review Applied*, 26(1):014028, 2026.

[39] AB Zorin. Josephson traveling-wave parametric amplifier with three-wave mixing. *Physical Review Applied*, 6(3):034006, 2016.

[40] Chris Macklin, K O'brien, D Hover, ME Schwartz, V Bolkhovsky, X Zhang, WD Oliver, and I Siddiqi. A near–quantum-limited josephson traveling-wave parametric amplifier. *Science*, 350(6258):307–310, 2015.

[41] Kevin O'Brien, Chris Macklin, Irfan Siddiqi, and Xiang Zhang. Resonant phase matching of josephson junction traveling wave parametric amplifiers. *Physical review letters*, 113(15):157001, 2014.

[42] Zh. Wang, M. Xu, X. Han, W. Fu, Sh. Puri, S. M. Girvin, H. X. Tang, S. Shankar, and M. H. Devoret. Quantum microwave radiometry with a superconducting qubit. *Physical Review Letters*, 126:180501, 2021.

[43] O. Astafiev, A. M. Zagoskin, A. A. Abdumalikov Jr, Y. A. Pashkin, T. Yamamoto, K. Inomata, Y. Nakamura, and J. S. Tsai. Resonance fluorescence of a single artificial atom. *Science*, 327(5967):840–843, 2010.

[44] R. Sett, F. Hassani, D. Phan, S. Barzanjeh, A. Vukics, and J. M. Fink. Emergent macroscopic bistability induced by a single superconducting qubit. *PRX Quantum*, 5:010327, 2024.

[45] L. S. Bishop, E. Ginossar, and S. M. Girvin. Response of the strongly driven jaynes-cummings oscillator. *Physical Review Letters*, 105:100505, 2010.

[46] Á. Kurkó, N. Német, and A. Vukics. How is photon-blockade breakdown different from optical bistability? a neoclassical story. *Journal of the Optical Society of America B*, 41:C29, 2024.

[47] J. E. Mooij, T. P. Orlando, L. Levitov, L. Tian, C. H. Van der Wal, and S. Lloyd. Josephson persistent-current qubit. *Science*, 285(5430):1036–1039, 1999.

[48] T. P. Orlando, J. E. Mooij, L. Tian, C. H. Van Der Wal, L. S. Levitov, S. Lloyd, and J. J. Mazo. Superconducting persistent-current qubit. *Physical Review B*, 60(22):15398, 1999.

[49] P. Navez, E. Brambilla, A. Gatti, and L. A. Lugiato. Spatial entanglement of twin quantum images. *Physical Review A*, 65(1):013813, 2001.

[50] A. Roy and M. Devoret. Introduction to parametric amplification of quantum signals with josephson circuits. *Comptes Rendus Physique*, 17(7):740–755, 2016.

[51] P. Silvestrini, R. Russo, V. Corato, B. Ruggiero, C. Granata, S. Rombetto, M. Russo, M. Cirillo, A. Trombettoni, and P. Sodano. Topology-induced critical current enhancement in josephson networks. *Physics Letters A*, 370(5-6):499–503, 2007.

[52] J. Settino, G. G. Luciano, A. Di Bartolomeo, P. Silvestrini, M. Lisitskiy, B. Ruggiero, and F. Romeo. Topology-enhanced superconducting qubit networks for in-sensor quantum information processing. *Quantum Science and Technology*, 11(1):015019, 2026.

[53] P. Navez, A. G. Balanov, S. E. Savel'ev, and A. M. Zagoskin. Quantum electrodynamics of non-demolition detection of single microwave photon by superconducting qubit array. *Journal of Applied Physics*, 133(10), 2023.

[54] S. Probst, F. B. Song, P. A. Bushev, A. V. Ustinov, and M. Weides. Efficient and robust analysis of complex scattering data under noise in microwave resonators. *Review of Scientific Instruments*, 86:024706, 2015.

Acknowledgements

The authors thank E. Il'ichev and G. Oelsner for layout design and fabrication of samples in the Leibniz Institute of Photonic Technology , Jena, Germany. M.V.F acknowledge the hospitality and the partial financial support of the Center for Theoretical Physics of Complex Systems (PCS), Institute for Basic Science (IBS), Republic of Korea and the International Institute of Physics (IIP), Natal Brazil. This work was funded from the European Union's Horizon 2020 Research and Innovation Programme under Grant Agreement No. 863313 (SUPERGALAX) and is partially supported from the PNRR MUR projects National Center for HPC, Big Data and Quantum Computing – HPC (Centro Nazionale 01-CN0000013) and National Quantum Science and Technology Institute - NQSTI (Partenariato Esteso 04: Scienze e Tecnologie Quantistiche PE0000023), both funded from the European Union – NextGenerationEU.

Author contributions

P.N. developed the theoretical model based on Gross-Pitaevskii formalism, confirmed the theoretical prediction with experiment, wrote the theoretical part of the manuscript. V.D.M. analyzed the raw experimental data, participated in confirmation of experimental data with theory, wrote the experimental part of the manuscript and made preparation of the manuscript. B.R. contributed in the organization of the experiment, participated in the cryogenic measurements and in raw experimental data anal-

ysis, and in writing of the manuscript. C.G. participated in projecting of the sample, realized ultra low temperature microwave cryogenic setup, carried out the cryogenic measurements, performed preliminary experimental data analysis, contributed in the understanding of experimental result and their confirmation with theoretical prediction. F.C- designed the automatic data acquisition protocol, operated the cryogenic measurements. A.D.E. participated in the cryogenic measurements, performed preliminary analysis of raw experimental data. A.R participated in cryogenic measurements. G.B. contributed to analysis of the scattering parameter experimental data, participated in experimental loss parameter estimation of the resonator. E.E. contributed to realization of the ultra low temperature microwave cryogenic setup by projecting sample holder for microwave measurements, performed the experimental estimation of the loss parameter of the resonator. L.F. participated in the experimental estimation of the loss parameter of the resonator. M.F. participated in projecting of the sample, suggested measurements during experiment, proposed the idea to explain the bistability phenomenon, carried out the fitting of experimental data with his preliminary simulations, participated in many discussions about comparison of experimental data with theory. I.E and A.Z. contributed in development of theoretical model. P.V. made the fitting procedure for loss parameter estimation. P.S. made suggestion for loss parameter estimation, contributed in comparison experiment with theory and in writing of the paper. M.L. coordinated all activity, participated in projecting of the sample, contributed in the organization of the experiment, participated in the cryogenic measurements and in raw experimental data analysis, contributed in comparison experiment with theory, participated in writing of the manuscript.

All authors contributed to the understanding of the results and to writing of the manuscript.

Supplementary Files

This is a list of supplementary files associated with this preprint. Click to download.

- Supplementarymaterial.pdf